



A large and complete Jurassic geothermal field at Claudia, Deseado Massif, Santa Cruz, Argentina



Diego M. Guido ^{a,*}, Kathleen A. Campbell ^b

^a CONICET and Facultad de Ciencias Naturales y Museo, Universidad Nacional de La Plata, Instituto de Recursos Minerales (INREMI), Calle 64 y 120, La Plata (1900), Argentina

^b Geology, School of Environment, University of Auckland, Private Bag 92019, Auckland 1142, New Zealand

ARTICLE INFO

Article history:

Received 27 November 2013

Accepted 17 February 2014

Available online 24 February 2014

Keywords:

Cerro Vanguardia

Patagonia

Hot springs

Sinter

Travertine

Paleoenvironmental analysis

ABSTRACT

Late Jurassic geothermal deposits at Claudia, Argentinean Patagonia, are among the largest (40 km²) and most varied in the Deseado Massif, a 60,000 km² volcanic province hosting precious metals (Au, Ag) mineralization generated during diffuse back arc spreading and opening of the South Atlantic Ocean. Both siliceous sinter and travertine occur in the same stratigraphic sequence. Deposits range from those interpreted as fluvially reworked hydrothermal silica gels, to extensive apron terraces, to a clustering of high-temperature subaerial vent mounds. Paleoenvironmentally diagnostic textures of sinters include wavy laminated, bubble mat and nodular fabrics, and for travertines comprise fossil terracette rims, wavy laminated, bubble mat, spherulitic, oncoidal, and peloidal fabrics. Of special note is the presence of relatively large (to 25 cm high), inferred subaqueous “*Conophyton*” structures in travertines, which serve as analogs for some Precambrian stromatolites and imply the presence of relatively deep pools maintained by voluminous spring discharges. The Claudia geothermal field is geographically and geologically linked to the Cerro Vanguardia epithermal project (total resource of ~7.8 million ounces Au equivalent) via proximity, similar veins, and structural linkages, making it an especially large and relevant prospect for the region. The combined Claudia–Cerro Vanguardia hydrothermal system likely represents a fortuitous alignment of focused fluid flow and structure conducive to forming a giant epithermal ore deposit, with respect to size, ore concentration and potentially duration, in the Late Jurassic of Patagonia.

© 2014 Elsevier B.V. All rights reserved.

1. Introduction and regional setting

Terrestrial hot springs are of interest to geologists because they represent the shallowest portions of hydrothermal systems that may be related to geothermal energy reservoirs or epithermal mineral resources (e.g., Henley and Ellis, 1983; Goldie, 1985; Krupp and Seward, 1987; Rice and Trewin, 1988; White et al., 1989; Sillitoe, 1993; Zimmerman and Larson, 1994; Sherlock et al., 1995; Vikre, 2007; Guido and Campbell, 2011; Lynne, 2012). They also are important to paleontologists because their ecosystems contain organisms adapted to life at high temperatures (Brock, 1978; Rothschild and Mancinelli, 2001), which may become entombed in minerals precipitating from the discharging and cooling thermal fluids (e.g., Cady and Farmer, 1996; Walter et al., 1996; Trewin et al., 2003). The ensuing deposits thus have possible significance in studies of early life on Earth (e.g., Walter, 1972; Konhauser and Ferris, 1996; Konhauser et al., 2001, 2003). Moreover, hot springs are relevant to astrobiologists because hydrothermal systems commonly are cited as potential targets in the search for fossilized microbial life on Mars (e.g., Bock and Goode, 1996; Farmer and Des Marais, 1999; Des Marais et al., 2008; Committee on the Review of Planetary Protection

Requirements for Mars Sample Return Missions, 2009). In recent years, a rover mission has discovered siliceous deposits in a Martian volcanic setting, interpreted as fumarole- or hot spring-related (Squyres et al., 2008; Ruff et al., 2011).

Continental hot spring deposits on Earth are largely found in volcanic terrains in which shallow crustal magma serves as the heat source for hydrothermal fluids reaching the surface (Sillitoe, 1993; Tosdal et al., 2009). Beneath such high-temperature, mainly subaerial hydrothermal systems, gold and silver epithermal ores form at <2-km depths and <300 °C (White and Hedenquist, 1990; Simmons et al., 2005). Surface hot spring deposits may be composed of calcium carbonate (travertine) precipitated from bicarbonate fluids where sufficient Ca²⁺ is present, typically around the margins of geothermal fields (Renaut and Jones, 2011). In volcanic settings, bicarbonate fluids condense in shallow groundwaters from steam and CO₂ gas ascending from deep adiabatic boiling (Hedenquist and Browne, 1989; Hedenquist, 1990; White and Hedenquist, 1990; Yoshimura et al., 2004; Gibert et al., 2009). Some hot spring fluids may contain dissolved amorphous silica, forming siliceous sinter derived from alkali–chloride fluids tapping deep magmatic reservoirs (Henley and Ellis, 1983). Mixed acid–sulfate–chloride waters also occasionally deposit thin sinters and sulfate-bearing minerals (e.g., Jones et al., 2000a; Schinteie et al., 2007). Long-term preservation of microorganisms from these ‘extreme environments’

* Corresponding author. Tel./fax: +54 221 4225648.
E-mail address: diegoguido@yahoo.com (D.M. Guido).

is facilitated by rapid opaline silica mineralization (Cady and Farmer, 1996), or carbonate precipitation followed by early diagenetic silicification (e.g., Guido and Campbell, 2012). Whether microbial signatures and their enclosing hot spring deposits survive subsequent geological events is an important consideration (e.g., Simmons et al., 1993) and, indeed, fossil geothermal fields are rare in Mesozoic and older rocks (e.g., Rice and Trewin, 1988; Cuneen and Sillitoe, 1989; White et al., 1989; Sillitoe, 1993).

The Deseado Massif region (60,000 km²) is located in the southernmost part of Argentinean Patagonia (Santa Cruz province; Fig. 1). In the Middle–Late Jurassic (~178–151 Ma; Pankhurst et al., 2000), the Massif area was affected by mostly rhyolitic and andesitic volcanism owing to crustal thinning in a diffuse extensional back arc setting affiliated with the break-up of Gondwana and opening of the South Atlantic Ocean (Riley et al., 2001; Richardson and Underhill, 2002). Associated with the mature (quiescent) volcanic phase in the Late Jurassic was widespread hydrothermal activity, which produced metalliferous epithermal deposits (mainly Ag, Au), extensive silicification, and formation of geothermal fields at the surface (Schalamuk et al., 1997; Guido and Campbell, 2011). More than 50 Jurassic metalliferous occurrences are known from the Deseado Massif, mainly classified as the epithermal low sulfidation type (Schalamuk et al., 1997), including five mines and several others

under advanced development. During exploration and field reconnaissance surveys, numerous near-intact, fossilized geothermal fields have been found within volcanoclastic fluviolacustrine strata, distributed in a 400 × 250 km area of NW- or SE-oriented belts aligned with major regional structures (see Guido and Campbell, 2011, fig. 1, p. 37).

Based on modern hot spring analogs, such as Yellowstone National Park, U.S.A., and the Taupo Volcanic Zone (TVZ), New Zealand, diverse sedimentary facies types have been identified in Deseado Massif hot spring deposits (Guido and Campbell, 2011), several of which contain well-preserved prokaryote and eukaryote fossils (Guido and Campbell, 2009; Guido et al., 2010; Channing et al., 2011; Guido and Campbell, 2011; García Massini et al., 2012; Guido and Campbell, 2012). Geothermal paleoenvironments are defined by several stratigraphic, sedimentologic and paleontologic attributes (cf. Walter et al., 1996; Campbell et al., 2001; Pentecost, 2005; Guido and Campbell, 2011), controlled largely by spring discharge composition, hydrodynamics and temperature gradients from vent source areas (~100 °C) to surrounding geothermally influenced marshes (ambient) (Walter, 1976; Cady and Farmer, 1996; Lowe et al., 2001; Pentecost, 2005; Channing and Edwards, 2009).

This contribution describes a geographically extensive, Jurassic siliceous sinter and travertine deposit in the Deseado Massif province,

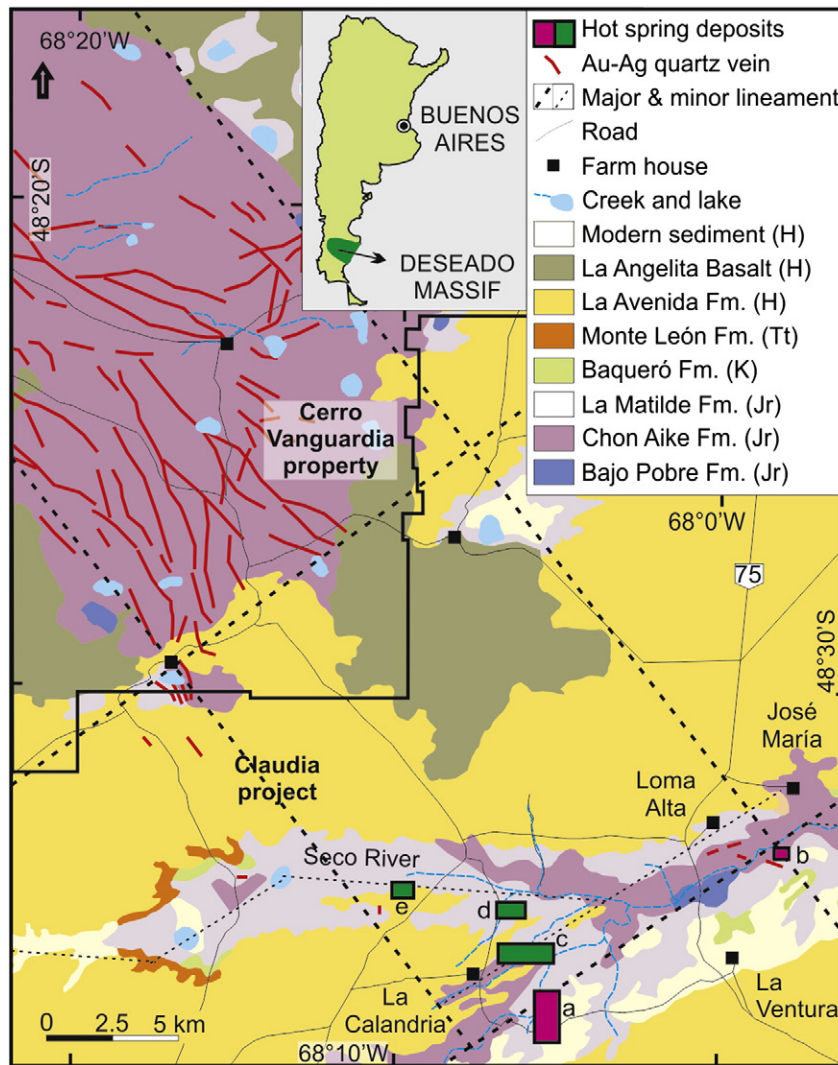


Fig. 1. Regional geological overview (from Panza et al., 1994), with addition of Cerro Vanguardia and Claudia epithermal veins and the Claudia hot spring outcrops (a = La Calandria Sur, b = Loma Alta, c = La Calandria Norte, d = Lote 8 Este, e = Lote 8). Red colored outcrops were studied in detail (see Figs. 2, 4) while green colored outcrops did not exhibit good preservation. Inset shows the location of the Deseado Massif volcanic province in the southern part of Argentina.

situated at the eastern end of the Southern Belt epithermal trend, as defined by Guido and Campbell (2011). The Claudia geothermal field is geologically related to the most significant, major, low sulfidation epithermal occurrence in the province, the Cerro Vanguardia world-class Au–Ag deposit (Fig. 1). Since 1998, Cerro Vanguardia has produced about 200,000 oz Au and 2 million ounces (Moz) Ag per annum, with reported mineral resources in 2012 of 4.72 Moz Au and 40 Moz Ag (AngloGold Ashanti, 2012). Thus, the total resource is approximately 7.8 Moz Au equivalent. Claudia is an epithermal exploration project that follows Jurassic veins to the south of Cerro Vanguardia, within the same structural trend, although the resource at Claudia is largely covered by younger geological units (Fig. 1). The implications of this discovery for characterizing the Cerro Vanguardia–Claudia epithermal system are discussed further in Section 3.

The Claudia hot spring deposit shows a distinctive stratigraphic intercalation of sinter and travertine/silicified travertine. It also contains the first sinter example from the Deseado Massif that archives all the different “classic” paleoenvironmental gradients (cf. Walter, 1976; Lowe et al., 2001) – from high temperature vent conduits to low temperature plant-rich facies. In comparison, the San Agustín sinter (Guido et al., 2010) lacks evidence for vent deposits because of subsequent faulting and erosion. The La Marciana sinter (Guido et al., 2002; Guido and Campbell, 2009) is missing the geothermally influenced marsh facies, typically the most volumetric and geographically extensive part of a geothermal field (Weed, 1889; Walter, 1976), owing to its removal in an active paleo-fluvial setting during the Late Jurassic, or due to more recent erosion.

2. Claudia geothermal field description

2.1. Overview of Claudia system distribution

Regionally the Claudia paleo-hydrothermal system is broadly characterized by geographically extensive travertine and silicified travertine sandwiched between localized siliceous sinter deposits, some of which appear to be vent-associated, which altogether demarcate diverse and widespread Late Jurassic geothermal activity. It was discovered by geologists working for mining companies (Mirasol Resources Ltd. and Hochschild Mining Argentina) and mapped during exploration of the area (Guido and Campbell, 2011), but has not been described in detail until now. It is located 20 km to the southwest of and in the same NW-oriented structural trend as the Cerro Vanguardia mine (Fig. 1).

Fig. 1 shows a regional overview of the Claudia structural block and its relationship to the Cerro Vanguardia structural block. The geology of the area is summarized from Panza et al. (1994) and comprises a Jurassic volcanic complex of three main formational units: the Chon Aike, Bajo Pobre and La Matilde formations (reviewed in Echeveste et al., 2001; Guido, 2004). The Jurassic volcanics are largely covered in the northerly Cerro Vanguardia block by Holocene basalts of the La Angelita Formation, and in the southerly Claudia block by local outcrops of Cretaceous sediments of the Baqueró Formation, and by basin-fill deposits of Cenozoic marine sediments (Monte León Fm) and Quaternary fluvio-glacial gravels (La Avenida Fm). The two structural blocks are separated by a large ENE lineament, parallel to the Seco river lineament ~17 km to the south, which also aligns with minor E–W faults. The blocks are bounded by NW lineaments, creating a horst and graben structural pattern. The Cerro Vanguardia horst block exposes older and structurally deeper rocks than the Claudia block, the latter of which appears to have been a basinal graben that filled with younger sediments. The major lineaments may have been active since the Jurassic, and even up to the Holocene, since the local young basalts appear to have flowed out from these structural features.

Five major outcrop areas (La Calandria Sur, Loma Alta, La Calandria Norte, Lote 8, Lote 8 Este: ~40 km² total area of fossil geothermal activity) constitute the group of exposed hot spring deposits at Claudia

(Fig. 1). They are located in an ENE erosive window of the modern day Seco River that exposes lower Jurassic and Cretaceous volcaniclastics, which are otherwise partially covered by younger Quaternary deposits. The Late Jurassic hot spring deposits are distributed along the E–W to ENE fault of the Río Seco lineament, and between the NNW major lineaments. Four outcrops occur to the west, and the Loma Alta outcrop is positioned to the east. Two of the sites display better preservation (La Calandria Sur and Loma Alta); hence, they were mapped and studied in detail (Figs. 2–4). The remaining outcrops also have distinctive features (Fig. 5), and are described briefly below.

2.2. La Calandria Sur outcrop

Fig. 2 shows the entire group of hot spring-related deposits comprising the La Calandria Sur locality (“a” in Fig. 1), exposed in a N–S oriented, 1.3-km-long series of outcrops (1300 m × 400 m total area) spatially associated with younger rhyolites and some pyroclastic deposits. The geothermal field was largely hosted within an interpreted siliciclastic lacustrine sedimentary sequence, with interbedded fluvial strata at its base (Fig. 2A). The southern outcrop area (Fig. 2A) is not well-preserved, and is mainly represented by widespread and large siliceous blocks with travertine textures that in their lower portions are still preserved as carbonate; hence, it was mapped as mainly a silicified travertine (pseudosinter; sensu Guido and Campbell, 2011). Silicified travertines can be distinguished from siliceous sinters by primary textural differences (Guido and Campbell, 2011, their fig. 3 and table 1, p. 40) and, for many pseudosinters, by distinctive paleo-weathered surfaces and lack of internal porosity (unpublished data).

The northern part of the La Calandria Sur area preserves a complete hot spring-related sequence (Fig. 2A–B) which, at its base, exhibits the same fluvial interbedding with lacustrine strata, containing small lenses and horizons (few cm’s thick) of discontinuous hydrothermal chert (Fig. 3A), representing the most distal areas of hydrothermal influence. As the lacustrine laminae are bent around the chert layers, it is clear that the cherts underwent early lithification, perhaps during infusion of hydrothermal fluids within sedimentary horizons, followed by differential compaction of the deposit. These strata are overlain by localized sinter, termed herein the Lower Sinter (~1.5 m thick; Fig. 2C). Textural and geomorphologic characteristics of the Lower Sinter imply that it is mainly a mid- to low temperature sinter apron. In particular, the outcrop is blocky and thickly bedded, with a wavy laminated fabric containing small conical tufts (to ~1 cm high; Fig. 3B) and amygdaloidal voids (Fig. 3C, i.e., trapped bubbles from photosynthetic degassing of cyanobacterial mats; Hinman and Lindstrom, 1996), inferred as mid-temperature channels (~40–55 °C) in a mid-apron setting. On its distal margins, the Lower Sinter is thinner (to 0.5 m thick), massive to crudely bedded, intercalated with fluvio-lacustrine strata, and contains abundant plant fragments (Fig. 3D). This portion of the Lower Sinter is interpreted as a transition from distal apron to geothermally influenced marsh facies. The Lower Sinter is oriented N–S, parallel to the overarching N–S lineament of the La Calandria Sur outcrop (Fig. 2A), which may demarcate a paleo-fracture zone as a source point for the discharge of geothermal fluids.

The Lower Sinter is overlain by travertine deposits, preserved as carbonate in their lower portions and silicified in their upper levels. The travertine (Fig. 3E–J) preserves varied textures which together are indicative of low- to mid-temperature, carbonate-spring apron terraces (cf. Guido and Campbell, 2011, 2012, and references therein), including terracette rims (Fig. 3E), wavy layered “bubble mats” with sponge-like porosity (Fig. 3F), spherulites (Fig. 3G), peloids and concentrically lined oncoids (Fig. 3H), large (up to 25 cm high) conical stromatolites (“*Conophyton*”, Fig. 3I), and an unusual worm-like fabric (Fig. 3J), the latter of which also occurs in the thermogene travertines at El Macanudo (unpublished data). The best preserved travertine fabrics at La Calandria Sur coincide with areas of partial to complete silicification.

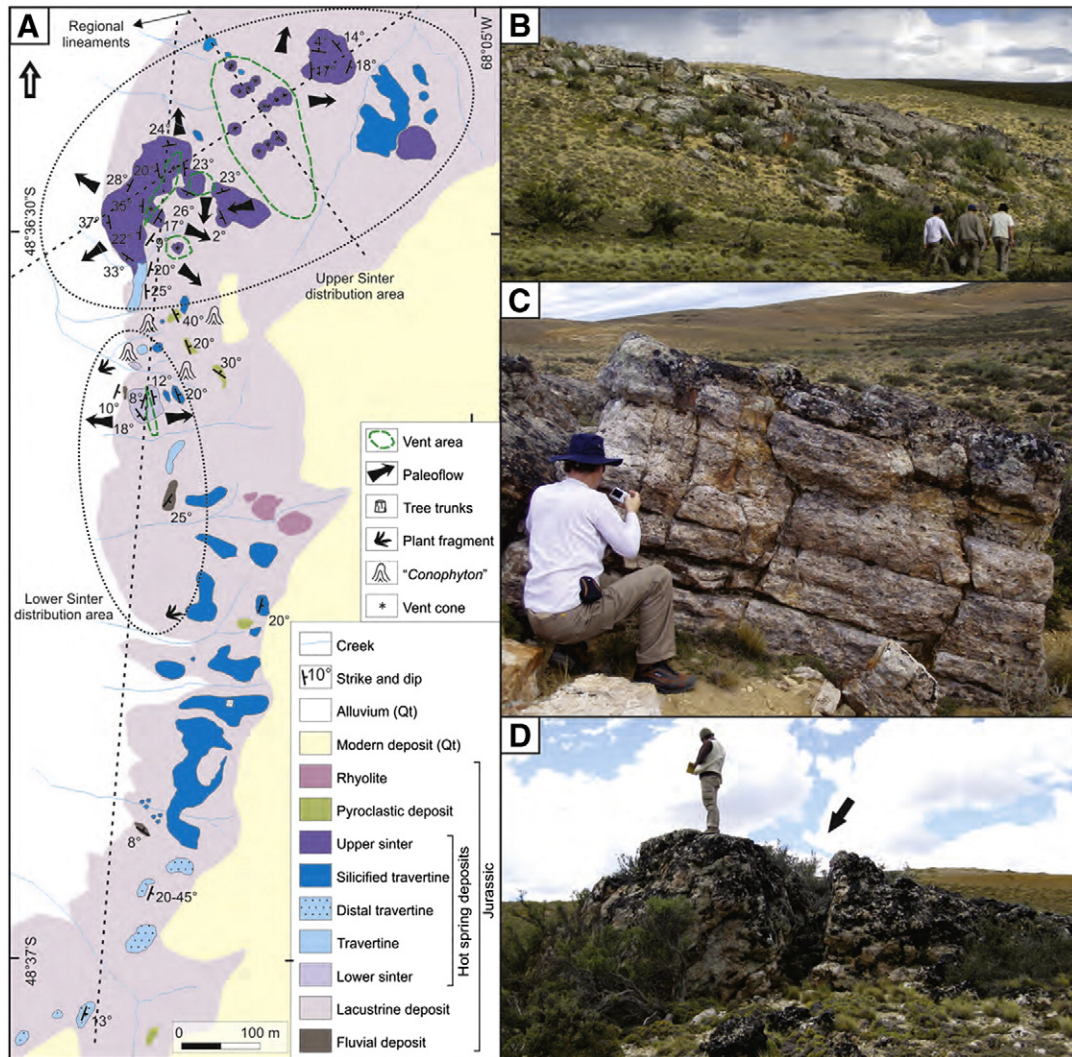


Fig. 2. La Calandria Sur outcrop. (A) Geological map showing the distribution of hot spring deposits, facies, vents and paleoflow directions. (B) View of the outcrops in the northern portion of La Calandria Sur, with lacustrine and fluvial deposits at the base, overlain by sinter with travertines. (C) Blocky outcrop of the mid- to low-temperature sinter deposit from the Lower Sinter. (D) Silicified breccias found within possible vent areas, with inferred conduits (arrow), from the Upper Sinter.

The travertines are overlain by more sinter deposits, termed Upper Sinter (Fig. 2A), which correspond with the topographically higher part of the La Calandria Sur outcrop area. They constitute thin aprons (to ~0.5 m thick) of low- to mid-temperature sinter (Fig. 2A, B) that are dotted with more than a dozen broadly circular siliceous mounds (up to 2.5 m high, up to 9 m diameter) cored in hydrothermal breccia (Fig. 3K), and which commonly display vertical hollow features (variably ~0.5 m diameter; Fig. 2D). The hollows are inferred as conduits and, in places, preserve possible nodular geyseritic textures on their surfaces (Fig. 3L) that likely indicate high-temperature vent deposits. The conduits are mainly affiliated with NW and NE lineaments, possibly related to deep faults that controlled fluid ascent. Detailed mapping and measurement of strikes and dips of in situ, laminated, Lower and Upper sinter outcrops enabled delineation of possible paleo-flow directions of the discharging geothermal fluids radially away from inferred vent areas (Fig. 2A).

2.3. Loma Alta outcrop and subcrop

The Loma Alta sinter occurrence is interbedded with the Jurassic volcanic Bahía Laura Complex in a low relief area on the margin of the Seco River ("b" in Figs. 1, 4A). The total area covered by hot spring deposits is 150 m × 50 m in an E–W direction. The sinter is located at

the intersection of two major faults: an E–W to ENE fault that controls the location of the Seco River, and a NW fault that constitutes the eastern border of the Cerro Vanguardia structural horst (Fig. 1). Outcrops at this locality are few and situated in the western part; the eastern area is represented by sinter subcrop or ex situ sinter blocks associated with fluvially reworked volcanoclastic sediments (Fig. 4A, B).

Three main hydrothermal facies were recognized in the Loma Alta hot spring deposit: high-temperature sinter, mid- to low-temperature sinter, and a late hydrothermal breccia (Fig. 4C–J). The high-temperature sinter is represented by an inferred columnar geyseritic fabric (Fig. 4C), and was found as float blocks in the northern and eastern parts of the outcrop area. The mid- to low-temperature sinter dominates in the western part of the outcrop area, and is composed of massive to faintly laminated silica layers that are parallel to slightly undulatory to wavy in morphology, and contain lenticular voids (bubble mats; Fig. 4D). A few poorly preserved plant fragments (Fig. 4E) can be found in this facies. This sinter fabric is interpreted to have formed in mid-temperature shallow channels and small pools positioned on a distal sinter apron that was possibly devoid of vegetation (cf. Campbell et al., 2001; Guido and Campbell, 2009, 2011). The wavy laminated sinter contains small conical tufts of similar size (to 1 cm high; Fig. 4F, G). Filamentous microbial fossils, in places densely and vertically packed within banded laminae (250–500 μm thick), are preserved in some of the wavy layers (Fig. 4H, I). Subsequent

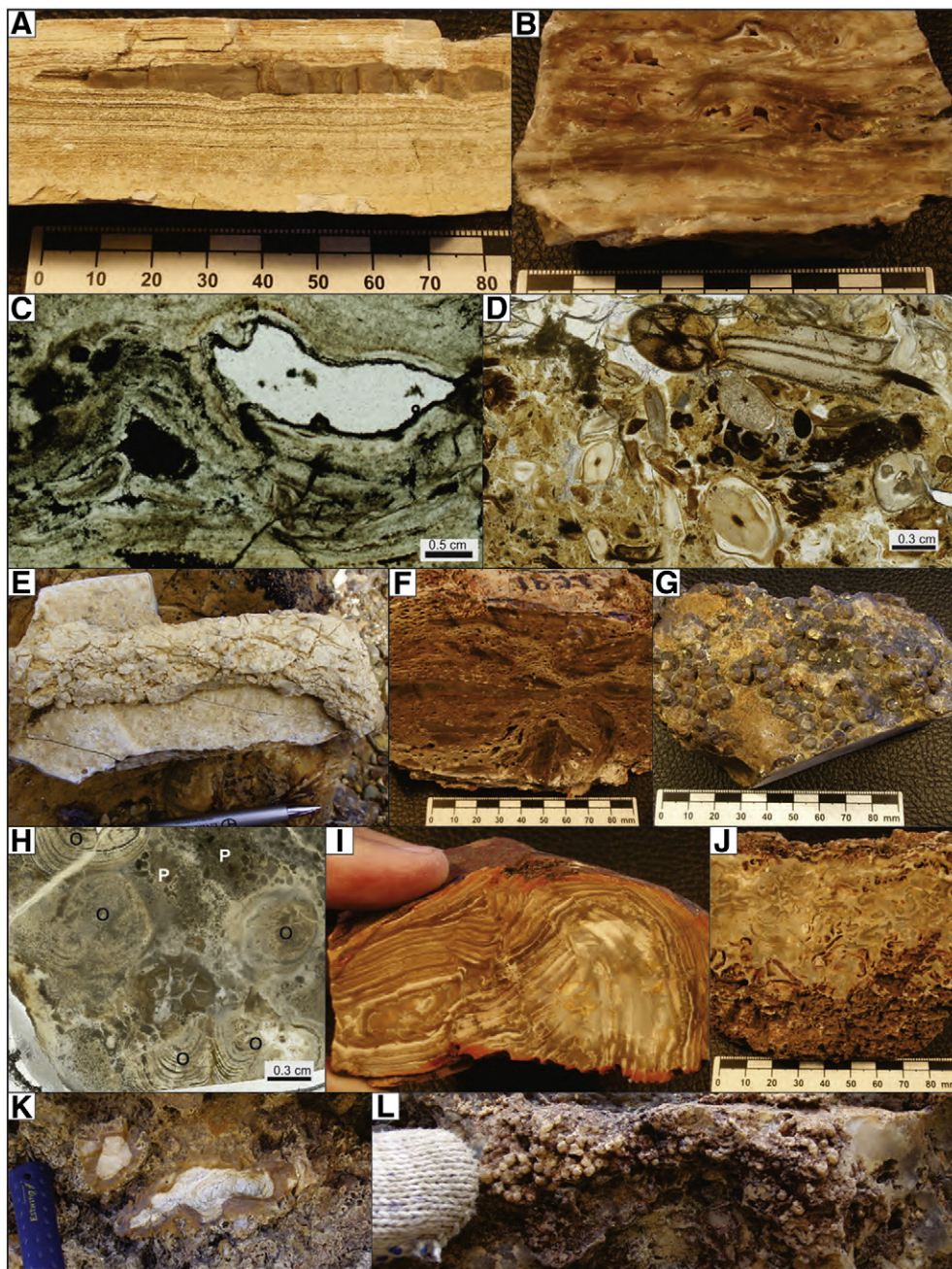


Fig. 3. La Calandria Sur outcrop. (A) Hydrothermal chert lenses (dark gray) in thin horizons of lacustrine sediments. (B) Mid-temperature sinter with bubble mats and conical tufts (cf. [Walter et al., 1976](#); [Hinman and Lindstrom, 1996](#)), Lower Sinter. (C) Photomicrograph of bubble mats with voids, Lower Sinter. (D) Plant-rich chert from the Lower Sinter. (E) Preserved terracette rim in travertine. (F) Travertine with porous sponge-like texture and bubble mats. (G) Spherulites in travertine (cf. [Farmer, 2000](#)). (H) Detail of oncoids (O) and peloids (P) in travertine, suggestive of low-temperature, distal apron terracette pools filled with fecal material of eukaryotes and clotted microbial fabrics (cf. [Walter, 1976](#); [Cady and Farmer, 1996](#)). (I) “*Conophyton*” in travertine (cf. [Walter et al., 1976](#)). (J) Worm-like fabric in travertine. (K) Breccia found at the base of the high temperature facies in the Upper Sinter. (L) Possible nodular geyseric texture in the Upper Sinter vents.

to deposition, an explosive hydrothermal event fragmented the sinter and produced a breccia with angular, mid-temperature sinter blocks in an oxidized, iron-rich silica matrix ([Fig. 4J](#)).

Detailed mapping and measurement of strikes and dips of the in situ laminated sinter determined possible paleo-flow directions of the discharging geothermal fluids ([Fig. 4A](#)). The hot spring fluids are interpreted to have flowed to the east in the mid-temperature facies area, and to the NNE in the mid- to low-temperature facies. Both orientations are in agreement with a vent area in the proximity of the breccia facies area. This breccia event could have been related to temporal sealing of hydrothermal fractures to produce overpressures and late brecciation of the sinter apron. The presence of float material of high-

temperature sinter facies in the northwestern area of the field has two potential explanations. Blocks could have been transported northeastward from a higher paleotopography in the SW, now eroded, similar to the occurrence of landslide blocks of geysericites developed today at the Te Kopia geothermal field in the TVZ ([Murphy, 2013](#)). Alternatively the clasts of Loma Alta geyseric material may be interpreted as broken, local remnants of low-relief vent-pool rims, i.e. where small hot springs subsequently may have developed locally through the mid-distal apron part of the field. Such high-temperature spring ‘point sources’ are common in Yellowstone and TVZ geothermal areas today, and produce only areally limited, ring-like geysericite deposits (e.g., [Braunstein and Lowe, 2001](#)).

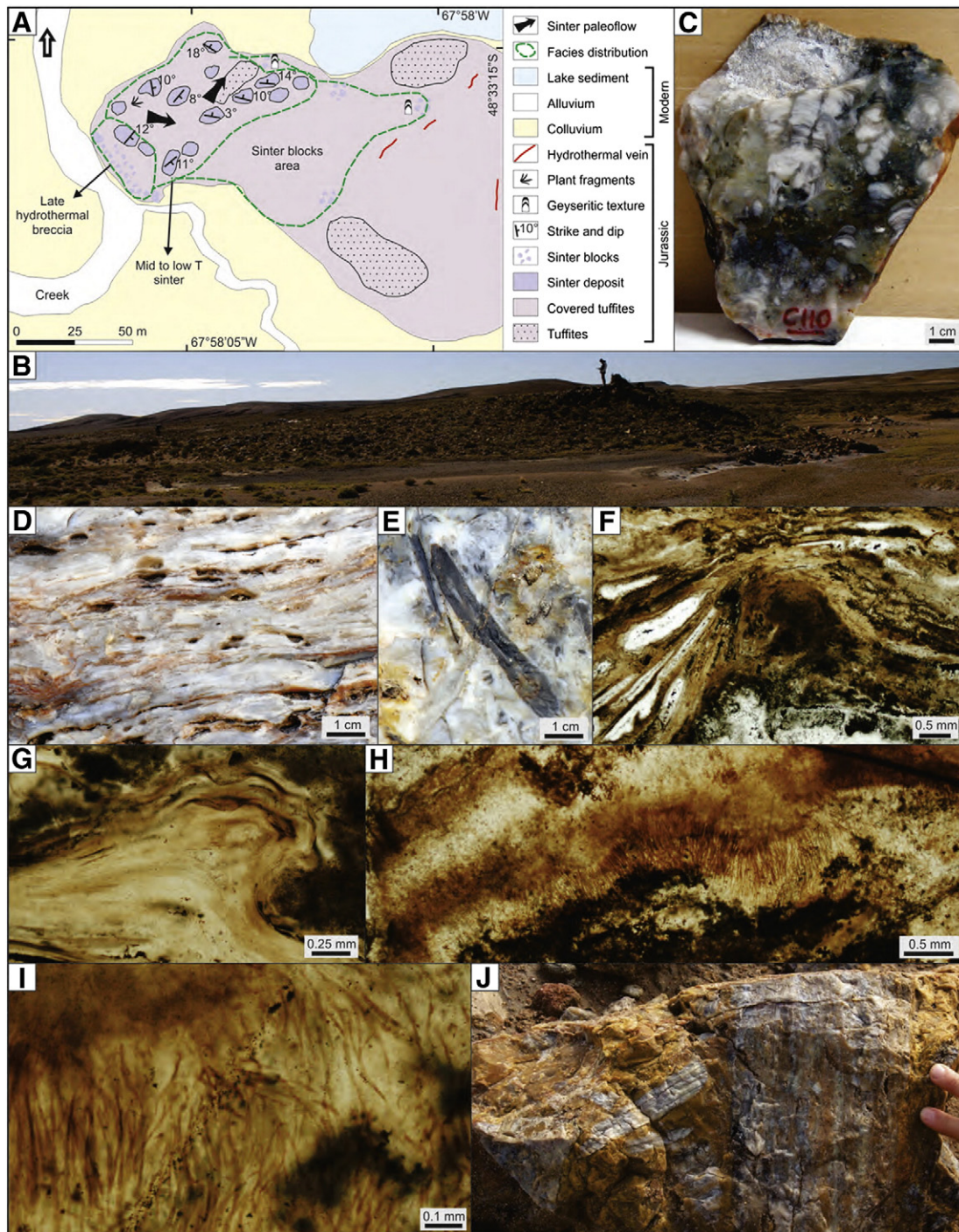


Fig. 4. Loma Alta outcrop. (A) Geological map showing distribution of hot spring deposits, facies, vents and paleoflow directions. (B) Overview of the Loma Alta outcrop. (C) Columnar geyseritic fabric found in blocks in the eastern outcrops. (D) Mid-temperature sinter with bubble mat (amygdaloidal porosity) in the western outcrops. (E) Low temperature sinter with scarce plant fragments. (F & G) Photomicrographs of bubble mats (white, quartz-filled lenticular voids) and conical tufts in dark laminated sinter. (H & I) Microbial filaments in sinter laminae. (J) Hydrothermal breccia with sinter clasts and Fe-rich matrix.

2.4. Other outcrops of hot spring deposits at Claudia

The other three outcrops at Claudia (“c–e” in Fig. 1) are not so well preserved, but some distinctive features and textures merit description here (Fig. 5). At the La Calandria Norte outcrop, a dominantly mid-temperature sinter is evident (e.g. Fig. 5A, wavy laminated fabric with lenticular voids). There also are remnants of silica-replaced travertine exposed in the lower part of the sequence, now a pseudosinter. In the northern part of the outcrop, some poorly preserved, irregularly circular vent breccias with conduits are found (Fig. 5B), some of which exhibit

proximal discharge channels traversing the slopes of the vent cones (Fig. 5C). At the Lote 8 Este outcrop, several types of hot spring deposits occur, including pseudosinter (Fig. 5D–F, wavy laminated fabric with lenticular voids), and localized patches of inferred high-temperature sinter with nodular geyseritic texture (Fig. 5G). Finally, the Lote 8 outcrop constitutes an unusual silicified fluvial conglomerate (Fig. 5H) with a brown-colored, wavy laminated, siliceous mudstone matrix into which light gray-colored, contorted, massive siliceous clasts are set (Fig. 5I, J). We interpret the light-colored clasts as silica gel originating on a discharge apron, and then washed into a subaqueous setting

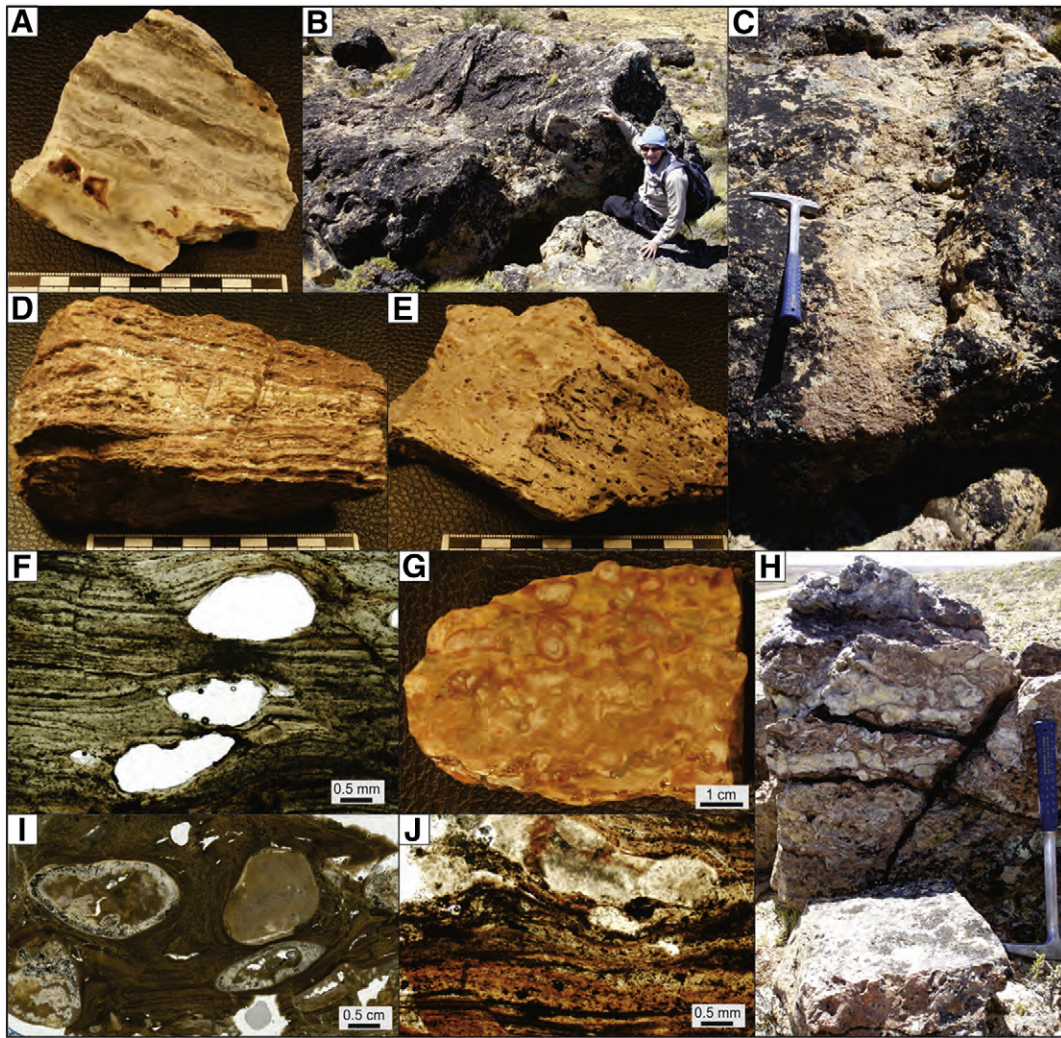


Fig. 5. Features found at other outcrops in the Claudia geothermal area. (A) Wavy laminated siliceous sinter from La Calandria Norte. (B) Vent and (C) possible vent channel from La Calandria Norte. (D, E & F) Silica replaced travertine, or pseudosinter, with sponge-like texture (E) and voids (F) from Lote 8 Este. How the porosity was maintained is not known but possibly reflects gaseous build up or conduits within the deposit during formation and lithification. (G) Possible high-temperature sinter with nodular geyseric texture from Lote 8 Este. (H, I & J) Fluvial conglomerate with possible silica gel clasts (light gray) set in a laminated, brown siliceous mudstone matrix from Lote 8.

when they were only partly solidified. However, the conglomerate requires further analysis to verify its formation mechanism.

3. Discussion

3.1. Paleoenvironmental character of the Claudia geothermal field

There are several distinctive attributes of Claudia's geothermal deposits that warrant further discussion with respect to their paleoenvironmental significance. In particular, Claudia is the only known hydrothermal system in the Deseado Massif that preserves interbedded sinter and travertine. In some modern geothermal areas, silica and carbonate co-precipitate at a local scale, such as at Ohaaki Pool, Waikite and Ngatamariki in the TVZ (Jones et al., 1998, 2000b; Campbell et al., 2002), but these preserve microscopic rather than bedding-scale shifts in lithology. In present day geothermal settings, silica and carbonate may co-precipitate from the same fluid without a change in fluid composition (Allen, 1934; Campbell et al., 2002), controlled by factors such as temperature of precipitation or location within the geothermal system (Renaut and Jones, 2011).

The Claudia geothermal field was not only large but also was probably long lived, experiencing many hydrothermal pulses over the history

of its development. In addition, subaerial sinter and travertine aprons appear to have been produced from discharge of large volumes of hot water, e.g. at La Calandria Sur (Section 2.2). This inference is based on several lines of evidence. First, apron outcrops cover a large area, which may indicate longevity of the system and/or a high discharge rate. Second, tall "Conophyton" stromatolites imply formation in relatively deep (>0.5 m) terrace pools (cf. Walter et al., 1976), similar to those found today growing on the mid-temperature sinter apron at Fountain Paint Pots, Lower Geyser Basin, Yellowstone, U.S.A. (Campbell, pers. obs.). Third, numerous vents occur at the top of the La Calandria Sur Upper Sinter deposit. The clustering of vents over an extended area (100 × 150 m), and large aprons situated topographically and stratigraphically beneath the paleo-vents, is a configuration comparable in size and facies distributions to the modern Clepsydra/Fountain/Red geyser group and its extensive sinter apron at Fountain Paint Pots in Yellowstone. It is exceptional that the La Calandria deposits preserve a complete paleo-temperature gradient sequence, from vent to apron to distal margin, as vents in particular are quite rare in fossil geothermal fields. Finally, the overall excellent preservation of silicified travertine and siliceous sinter fabrics at La Calandria Sur, including plants and microbial filaments, also attests to the widespread availability of thermal waters in which the contents of channels and terrace pools could be

rapidly preserved. In contrast, subaerial settings readily erode and weather sinters and especially travertines (Guido and Campbell, 2011). Indeed, the two conditions necessary to achieve maximum quality of organism preservation in hot spring deposits are constancy in thermal fluid availability and localized subaqueous mineralization within an overall subaerial environment on travertine and sinter terraces (Fouke, 2001; Trewin et al., 2003).

The Claudia geothermal field preserves abundant, large (to 25 cm high), strongly coniform, and distinctly and evenly laminated stromatolites in travertine that is commonly silicified (Fig. 31). These bear a striking resemblance to some Precambrian *Conophyton* (e.g., Schopf and Sovietov, 1976, fig. 2C, p. 145; Shixing, 1982, fig. 6D, p. 374), and large complex cone stromatolites (Allwood et al., 2009, fig. 4C, p. 9952), that formed in submarine paleoenvironments (e.g., Donaldson, 1976; Kah et al., 2009). For example, Donaldson (1976) noted the extremely uniform and persistent lamination in Precambrian subtidal examples from Canada, probably owing to minimal disturbance in relatively quiet subaqueous settings. Even parallel-lamination is a textural characteristic also observed in the Claudia fossils. Moreover, Walter et al. (1976) suggested a resemblance of mid-temperature, terrace-pool stromatolites forming at Yellowstone National Park to Precambrian stromatolites, including “*Conophyton*,” albeit on a much smaller scale in modern geothermal settings. The Late Jurassic Claudia “*Conophyton*” features grew to greater heights than the modern Yellowstone examples, and thus are more closely akin to the Precambrian forms, and they also occur in silica-replaced carbonates as in some Precambrian examples (e.g., Schopf and Sovietov, 1976). Thus, the Jurassic Patagonian examples appear to have analogous morphology and structure in comparison with the much older microbial features.

3.2. Regional geological relationships and the size and structure of the Claudia hydrothermal system

Fig. 6 shows the locations of the 23 known hot spring deposits of the Deseado Massif (Guido and Campbell, 2011), as well as regional aeromagnetic data (Chernicoff and Vargas, 1998) for the southern portion, which highlight the location of regional fractures controlling fluid ascent. From this figure it is clear that Claudia is located at the intersection of the Southern Belt and two major magnetic lineaments. In the Deseado Massif, a belt is defined as the combined product of distinct magnetic lineaments containing five or more aligned hot spring localities (Guido and Campbell, 2011). In the study area, the NNW lineament links Claudia deposits to the Cerro Vanguardia mine; whereas, the NNE major lineament is the most visually distinctive lineament observed on the geophysical map. The three directions are in agreement with regional large scale structures of the Middle to Upper Jurassic as defined by Giacosa et al. (2010). Regionally the Southern Belt hosts the majority of the silica-rich hot spring deposits in a province that is dominated by travertine (Guido pers. obs.). These silica-rich deposits include La Bajada plant-rich chert (Guido pers. obs.), La Marciana sinter (Guido and Campbell, 2009), La María plant-rich chert (Moreira et al., 2008), Cerro Vanguardia siliceous blocks (as yet unstudied; Guido and Campbell pers. obs.), and the Claudia sinters and travertines described in this contribution.

Geographic proximity and alignment with regional NW lineaments suggest a geological relationship between the Late Jurassic Claudia geothermal field (i.e. representing the surface expression of hydrothermal activity) and the world-class Cerro Vanguardia epithermal vein field – the most important gold and silver mine in the region, which is also hosted in the subsurface fluid plumbing of a paleo-geothermal field

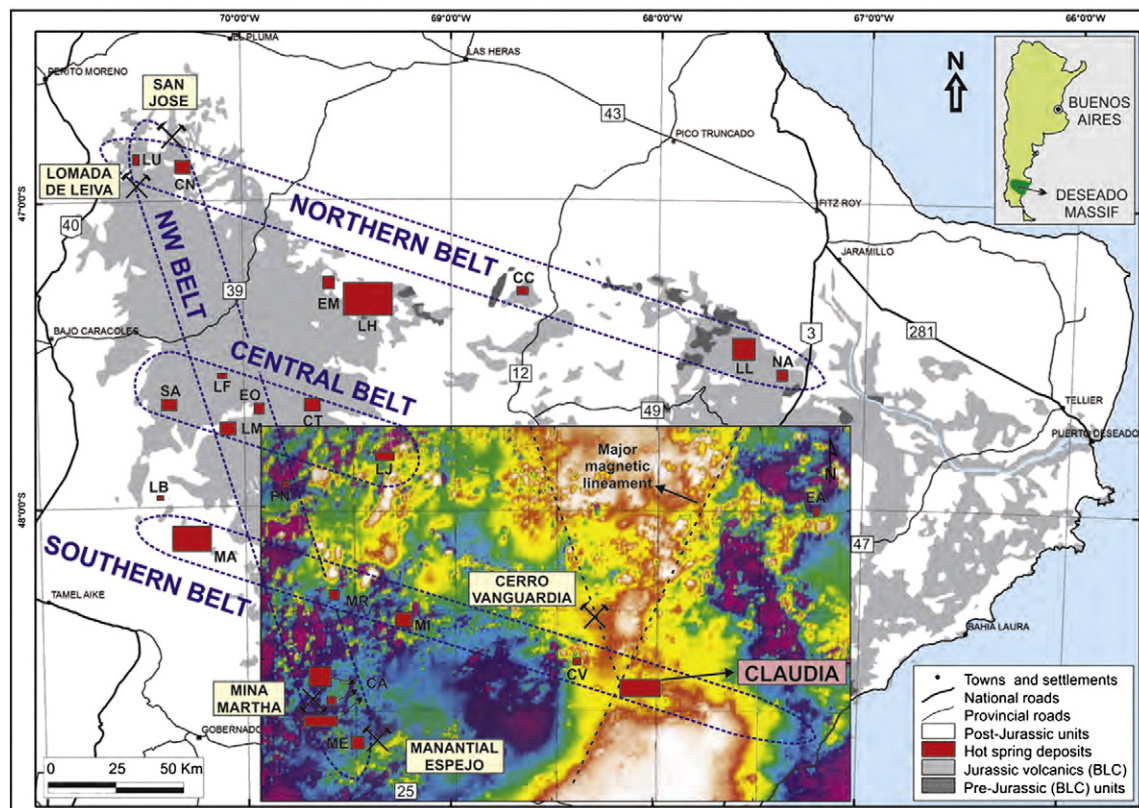


Fig. 6. Simplified geological map of the Deseado Massif with locations of the 23 known hot springs deposits. The Claudia hot spring area is located at the intersection of three major structures: the Southern Belt, a major hydrothermal-structural belt proposed by Guido and Campbell (2011), and two major magnetic anomalies (inferred as lineaments) defined by interpretation of the RTP (reduced to pole) magnetic map sourced from SEGEMAR (Chernicoff and Vargas, 1998). The other 22 hot spring localities are: LU: La Unión, CN: Cerro Negro, CC: Cerro Contreras, LH: La Leona, NA: Cañadón Nahuel, EM: El Macanudo, LH: La Herradura, EA: El Águila, SA: San Agustín, LF: La Flora, LM: La Marcelina, EO: Esperanza Oeste, CT: Cerro Tornillo, LJ: La Josefina, FN: Flecha Negra, LB: La Bajada, MA: La Marciana, MR: La María, MI: Monte Illiria, CV: Cerro Vanguardia, CA: Cerro 1 Abril, and ME: Manantial Espejo.

(Fig. 1). We also note that the best preserved hot spring outcrops at Claudia are those two of the five (La Calandria Sur and Loma Alta) that are situated in the southernmost area along NW-oriented lineaments, and in particular where these NW structures cross ENE fractures running parallel to the Seco River. We speculate that there could have been a general NW dipping tilt in the sequence to produce better preservation in the south, and exposure of deeper portions of the geothermal field to the north. Furthermore, the northern Claudia system contains similar Au–Ag epithermal veins to those at Cerro Vanguardia. The ENE regional lineament of the Seco River (Fig. 1), as interpreted from satellite images, may host a post-mineralization fault that produced broad block-segmentation through the greater epithermal area of Cerro Vanguardia and Claudia. These inferred associations between the epithermal Cerro Vanguardia deposits and the geothermal Claudia field require quantitative investigation and, at present, serve as an exploration hypothesis needing further testing.

The large size of the outcrop area of the Claudia hot spring deposits (about 40 km²) is only an indication of what actually may be present, since most of the Claudia project is covered by Holocene rocks (Fig. 1). Consequently, and due to its possible relationship with the largest vein field of the province, the Claudia hot spring deposit itself appears to be one of the largest of the Massif, with most of its geothermal features aligned with the regional WNW Southern Belt (Fig. 6). This hypothesis is supported by the presence of additional hot spring outcrops in the southwestern part of the Cerro Vanguardia district (Guido and Campbell, 2011; shown here in Fig. 6 as “CV”), which also are situated in the same regional belt with Claudia. In other parts of the world, Richards (2013) has observed that giant epithermal ore deposits – significant in relation to their geographic spread, duration and/or total ore concentration – largely form by optimal alignments and combinations of otherwise normal geological processes (e.g., distinctive tectonic configurations, high volume and/or intensity of focused fluid flow). The proposed Claudia–Cerro Vanguardia epithermal suite could qualify as just such a prodigious fossil hydrothermal system active during the Late Jurassic in Patagonia.

Acknowledgments

We gratefully acknowledge the National Geographic Society, INREMI (Instituto de Recursos Minerales), and the University of Auckland's Faculty Research Development Fund for financial and other support of this project. Mirasol Resources supplied the original field data that allowed us to work on the Claudia deposits, while the Hochschild Mining Argentina Company granted access permission for field work on the mining property.

References

- Allen, E.T., 1934. The agency of algae in the deposition of travertine and silica from thermal waters. *Am. J. Sci.* 27, 373–389.
- Allwood, A.C., Grotzinger, J.P., Knoll, A.H., Burch, I.W., Anderson, M.S., Coleman, M.L., Kanik, I., 2009. Controls on development and diversity of Early Archean stromatolites. *PNAS* 106, 9548–9555.
- AngloGold Ashanti, 2012. Mineral Resource and Ore Reserve Report. (182 pp. <http://www.aga-reports.com/12/>).
- Bock, G.R., Goode, G.A. (Eds.), 1996. *Evolution of Hydrothermal Ecosystems on Earth (and Mars?)*: Proceedings of the Ciba Foundation Symposium, 202. J. Wiley, Chichester (334 pp.).
- Braunstein, D., Lowe, D.R., 2001. Relationship between spring and geyser activity and the deposition and morphology of high temperature (>73 °C) siliceous sinter, Yellowstone National Park, Wyoming, U.S.A. *J. Sediment. Res.* 71, 747–763.
- Brock, T.D., 1978. *Thermophilic Microorganisms and Life at High Temperatures*. Springer-Verlag, New York (465 pp.).
- Cady, S.L., Farmer, J.D., 1996. Fossilization processes in siliceous thermal springs: trends in preservation along thermal gradients. In: Bock, G.R., Goode, G.A. (Eds.), *Evolution of Hydrothermal Ecosystems on Earth (and Mars?)*: Proceedings of the Ciba Foundation Symposium, 202. J. Wiley, Chichester, pp. 150–173.
- Campbell, K.A., Sannazzaro, K., Rodgers, K.A., Herdianita, N.R., Browne, P.R.L., 2001. Sedimentary facies and mineralogy of the Late Pleistocene Umukuri silica sinter, Taupo volcanic zone, New Zealand. *J. Sediment. Res.* 71, 728–747.
- Campbell, K.A., Rodgers, K.A., Brotheridge, J.M.A., Browne, P.R.L., 2002. An unusual modern silica–carbonate sinter from Pavlova spring, Ngatamariki, New Zealand. *Sedimentology* 49, 835–854.
- Channing, A., Edwards, D., 2009. Silicification of higher plants in geothermally influenced wetlands: Yellowstone as a Lower Devonian Rhynie analog. *Palaios* 24, 505–521.
- Channing, A., Zamuner, A., Edwards, D., Guido, D., 2011. *Equisetum thermale* sp. nov. (Equisetales) from the Jurassic San Agustín hot spring deposit, Patagonia, Argentina: anatomy, paleoecology, and inferred paleoecophysiology. *Am. J. Bot.* 98, 680–697.
- Chernicoff, C.J., Vargas, D., 1998. Levantamiento geofísico aéreo (magnetometría y espectrometría de rayos gamma) del Macizo del Deseado, Santa Cruz, República Argentina. Serie Contribuciones Técnicas, GeofísicaBancodeDatos, 2. SEGEMAR (18 pp.).
- Committee on the Review of Planetary Protection Requirements for Mars Sample Return Missions, 2009. *Assessment of Planetary Protection Requirements for Mars Sample Return Missions*. Space Studies Board, Division on Engineering and Physical Sciences, National Research Council of the National Academies, National Academy Press, Washington D.C. (80 pp.).
- Cuneen, R., Sillitoe, R.H., 1989. Paleozoic hot spring sinter in the Drummond Basin, Queensland, Australia. *Econ. Geol.* 84, 135–142.
- Des Marais, D., Nuth III, J.A., Allamandola, L.J., Boss, A.P., Farmer, J.D., Hoehler, T.M., Jakosky, B.M., Meadows, V.S., Pohorille, A., Runnegar, B., Spormann, A.M., 2008. The NASA astrobiology roadmap. *Astrobiology* 8, 715–730.
- Donaldson, J.A., 1976. Paleogeology of *Conophyton* and associated stromatolites in the Precambrian Dismal Lakes and Rae Groups, Canada. In: Walter, M.R. (Ed.), *Stromatolites*. Elsevier, Amsterdam, pp. 523–524.
- Echeveste, H., Fernandez, R., Bellieni, G., Tessone, M., Llambias, E., Schalamuk, I., Piccirillo, E., Demin, A., 2001. Relaciones entre las Formaciones Bajo Pobre y Chon Aike (Jurásico medio a superior) en el área de Estancia El Fénix–Cerro Huemul, zona centro-occidental del Macizo del Deseado, provincia de Santa Cruz. *Rev. Asoc. Geol. Argent.* 56, 548–558.
- Farmer, J.D., 2000. Hydrothermal systems: doorways to early biosphere evolution. *GSA Today* 10, 1–9.
- Farmer, J.D., Des Marais, D.J., 1999. Exploring for a record of ancient martian life. *J. Geophys. Res. Planets* 104 (E11), 26977–26995.
- Fouke, B.W., 2001. Depositional facies and aqueous–solid geochemistry of travertine-depositing hot springs (Angel Terrace, Mammoth Hot Springs, Yellowstone National Park, U.S.A.)—reply. *J. Sediment. Res.* 71, 497–500.
- García Massini, J., Channing, A., Guido, D.M., Zamuner, A.B., 2012. First report of fungi and fungus-like organisms from Mesozoic hot springs. *Palaios* 27, 55–62.
- Giacosa, R., Zubia, M., Sánchez, M., Allard, J., 2010. Meso-Cenozoic tectonics of the southern Patagonian foreland: structural evolution and implications for Au–Ag veins in the eastern Deseado region (Santa Cruz, Argentina). *J. South American Earth Sci.* 30, 134–150.
- Gibert, R.O., Taberner, C., Sáez, A., Giralt, S., Alonso, R.N., Edwards, R.L., Pueyo, J.J., 2009. Igneous origin of CO₂ in ancient and recent hot-spring waters and travertines in the northern Argentinean Andes. *J. Sediment. Res.* 79, 554–567.
- Goldie, R., 1985. The sinters of Ohaaki and Champagne pools, New Zealand: possible modern analogues of the Hemlo gold deposit, northern Ontario. *Geosci. Can.* 12, 60–64.
- Guido, D.M., 2004. Subdivisión litofacial e interpretación del volcanismo jurásico (Grupo Bahía Laura) en el este del Macizo del Deseado, provincia de Santa Cruz. *Rev. Asoc. Geol. Argent.* 59, 727–742.
- Guido, D.M., Campbell, K.A., 2009. Jurassic hot-spring activity in a fluvial setting at La Marciana, Patagonia, Argentina. *Geol. Mag.* 146 (4), 617–622.
- Guido, D.M., Campbell, K.A., 2011. Jurassic hot spring deposits of the Deseado Massif (Patagonia, Argentina): characteristics and controls on regional distribution. *J. Volcanol. Geotherm. Res.* 203, 35–47.
- Guido, D.M., Campbell, K.A., 2012. Diverse subaerial and sublacustrine hot springs setting of the Cerro Negro epithermal (Jurassic, Deseado Massif), Patagonia, Argentina. *J. Volcanol. Geotherm. Res.* 229–230, 1–12.
- Guido, D., De Barrio, R., Schalamuk, I., 2002. La Marciana Jurassic sinter – implications for exploration for epithermal precious-metal deposits in the Deseado Massif, southern Patagonia, Argentina. *Trans. Inst. Min. Metall. (Sect. B Appl. Earth Sci.)* 111, B106–B113.
- Guido, D.M., Channing, A., Campbell, K.A., Zamuner, A., 2010. Jurassic geothermal landscapes and fossil ecosystems at San Agustín, Patagonia, Argentina. *J. Geol. Soc. Lond.* 167, 11–20.
- Hedenquist, J.W., 1990. The thermal and geochemical structure of the Broadlands–Ohaaki geothermal system. *Geothermics* 19, 151–185.
- Hedenquist, J.W., Browne, P.R.L., 1989. The evolution of the Waiotapu geothermal system, New Zealand, based on the chemical and isotopic composition of its fluids, minerals and rocks. *Geochim. Cosmochim. Acta* 53, 2235–2257.
- Henley, R.W., Ellis, A.J., 1983. Geothermal systems ancient and modern: a geochemical review. *Earth Sci. Rev.* 19, 1–50.
- Hinman, N.W., Lindstrom, L.F., 1996. Seasonal changes in silica deposition in hot spring systems. *Chem. Geol.* 132, 237–246.
- Jones, B., Renaut, R.W., Rosen, M.R., 1998. Microbial biofacies in hot-spring sinters: a model based on Ohaaki Pool, North Island, New Zealand. *J. Sediment. Res.* 68, 413–434.
- Jones, B., Renaut, R.W., Rosen, M.R., 2000a. Stromatolites forming in acidic hot-spring waters, North Island, New Zealand. *Palaios* 15, 450–475.
- Jones, B., Renaut, R.W., Rosen, M.R., 2000b. Trigonal dendritic calcite crystals forming from hot spring waters at Waikite, North Island, New Zealand. *J. Sediment. Res.* 70, 586–603.
- Kah, L.C., Bartley, J.K., Stagner, A.F., 2009. Reinterpreting a Proterozoic enigma: *Conophyton–Jacutophyton* stromatolites of the Mesoproterozoic Atar Group, Mauritania. In: Swart, P.K., Eberli, G.P., McKenzie, J.A. (Eds.), *Perspectives in Carbonate Geology: A Tribute to the Career of Robert Nathan Ginsburg*. Special Publication of the International Association of Sedimentologists, 41, pp. 277–295.

- Konhauser, K., Ferris, F., 1996. Diversity of iron and silica precipitation by microbial mats in hydrothermal waters, Iceland: implications for Precambrian iron formations. *Geology* 24, 323–326.
- Konhauser, K.O., Phoenix, V.R., Bottrell, S.H., Adams, D.G., Head, I.M., 2001. Microbial-silica interactions in Icelandic hot spring sinter: possible analogues for some Precambrian siliceous stromatolites. *Sedimentology* 48, 415–433.
- Konhauser, K.O., Jones, B., Reysenbach, A.-L., Renaut, R.W., 2003. Hot spring sinters: keys to understanding Earth's earliest life forms. *Can. J. Earth Sci.* 40, 1713–1724.
- Krupp, R.E., Seward, T.M., 1987. The Rotokawa geothermal system, New Zealand: an active epithermal gold-depositing environment. *Econ. Geol.* 82, 1109–1129.
- Lowe, D.R., Anderson, K.S., Braunstein, D., 2001. The zonation and structuring of siliceous sinter around hot springs, Yellowstone National Park, and the role of thermophilic bacteria in its deposition. In: Reyensbach, A.M., Voytech, M., Mancinelli, R. (Eds.), *Thermophiles: Biodiversity, Ecology and Evolution*. Kluwer Academic/Plenum Publishers, New York, pp. 143–166.
- Lynne, B.Y., 2012. Mapping vent to distal-apron hot spring paleo-flow pathways using siliceous sinter architecture. *Geothermics* 43, 3–24.
- Moreira, P., Channing, A., de Barrio, R., Del Blanco, M., Fernández, R.R., Schalamuk, I.A., Zamuner, A., 2008. Fossil plants in hot spring rocks associated with a Jurassic epithermal environment in the central Deseado Massif, Argentinean Patagonia. 33rd International Geological Congress, Oslo, Norway, CD-Rom.
- Murphy, B.A., 2013. Siliceous Hotspring (Sinter) Deposits along the Paeroa Fault (TVZ): Archives of Geothermal Fluid History. Unpublished MSc Thesis, The University of Auckland, 163 pp.
- Pankhurst, R., Riley, T., Fanning, C.Y., Kelley, S., 2000. Episodic silicic volcanism in Patagonia and the Antarctic Peninsula: chronology of magmatism associated with the break-up of Gondwana. *J. Petrol.* 41, 605–625.
- Panza, J.L., Zubia, M.A., Genini, A.D., Godeas, M., 1994. Hoja Geológica 4949-II Tres Cerros, provincia de Santa Cruz. Secretaría de Minería de la Nación, Buenos Aires.
- Pentecost, A., 2005. *Travertine*. Springer, Berlin (445 pp.).
- Renaut, R.W., Jones, B., 2011. Hydrothermal environments, terrestrial. In: Reitner, J., Thiel, V. (Eds.), *Encyclopedia of Geobiology*. Springer, pp. 467–479.
- Rice, C.M., Trewin, N.H., 1988. A Lower Devonian gold-bearing hot spring system, Rhynie, Scotland. *Trans. Inst. Min. Metall. (Sect. B Appl. Earth Sci.)* 97, B141–B144.
- Richards, J.P., 2013. Giant ore deposits formed by optimal alignments and combinations of geological processes. *Nat. Geosci.* 6, 911–916.
- Richardson, N.J., Underhill, J.R., 2002. Controls on the structural architecture and sedimentary character of syn-rift sequences, North Falkland Basin, South Atlantic. *Mar. Pet. Geol.* 19, 417–443.
- Riley, T., Leat, P., Pankhurst, R., Harris, C., 2001. Origin of large volume rhyolitic volcanism in Antarctic Peninsula and Patagonia by crustal melting. *J. Petrol.* 42, 1043–1065.
- Rothschild, L.J., Mancinelli, R.L., 2001. Life in extreme environments. *Nature* 409, 1092–1101.
- Ruff, S.W., Farmer, J.D., Calvin, W.M., Herkenhoff, K.E., Johnson, J.R., Morris, R.V., Rice, M.S., Arvidson, R.E., Bell III, J.F., Christensen, P.R., Squyres, S.W., 2011. Characteristics, distribution, origin and significance of opaline silica observed by Spirit rover in Gusev crater, Mars. *J. Geophys. Res.* 116, E00F23.
- Schalamuk, I., Rubia, M., Genini, A., Fernández, R., 1997. Jurassic epithermal Au–Ag deposits of Patagonia, Argentina. *Ore Geol. Rev.* 12, 173–186.
- Schinteie, R., Campbell, K.A., Browne, P.R.L., 2007. Microfacies of stromatolitic sinter from acid-sulphate-chloride springs at Parariki stream, Rotokawa Geothermal Field, New Zealand. *Palaeontol. Electron.* 10 (1; 4A), 33.
- Schopf, J.W., Sovietov, Y.K., 1976. Microfossils in *Conophyton* from the Soviet Union and their bearing on Precambrian biostratigraphy. *Science* 193, 143–146.
- Sherlock, R.L., Tosdal, R.M., Lerhman, N.J., Graney, J.R., Losh, S., Jowett, E.C., Kesler, S.E., 1995. Origin of the McLaughlin mine sheeted vein complex: metal zoning, fluid inclusion, and isotopic evidence. *Econ. Geol.* 90, 2156–2181.
- Shixing, Z., 1982. An outline of studies on the Precambrian stromatolites of China. *Precambrian Res.* 18, 367–396.
- Sillitoe, R.H., 1993. Epithermal models: genetic types, geometrical controls and shallow features. In: Kirkham, R.V., Sinclair, W.D., Thorpe, R.I., Duke, J.M. (Eds.), *Mineral Deposits Modeling: Special Paper of the Geological Association of Canada*, 40, pp. 403–417.
- Simmons, S.F., Keywood, M., Scott, B.J., Keam, R.F., 1993. Irreversible change of the Rotomahana-Waimangu hydrothermal system (New Zealand) as a consequence of a volcanic eruption. *Geology* 21, 643–646.
- Simmons, S.F., White, N.C., John, D.A., 2005. Geological characteristics of epithermal precious and base metal deposits. In: Hedenquist, J.W., Thompson, J.F.H., Goldfarb, R.J., Richards, J.P. (Eds.), *Economic Geology 100th Anniversary Volume*, pp. 455–522.
- Squyres, S.W., Arvidson, R.E., Ruff, S., Gellert, R., Morris, R.V., Ming, D.W., Crumpler, L., Farmer, J.D., Des Marais, D.J., Yen, A., McLennan, S.M., Calvin, W., Bell III, J.F., Clark, B.C., Wang, A., McCoy, T.J., Schmidt, M.E., de Souza Jr., P.A., 2008. Detection of silica-rich deposits on Mars. *Science* 320, 1063–1067.
- Tosdal, R.M., Dilles, J.H., Cooke, D.H., 2009. From source to sinks in auriferous magmatic-hydrothermal porphyry and epithermal deposits. *Elements* 5, 289–295.
- Trewin, N.H., Fayers, S.R., Kelman, R., 2003. Subaqueous silicification of the contents of small ponds in an early Devonian hot spring complex, Rhynie, Scotland. *Can. J. Earth Sci.* 40, 1697–1712.
- Vikre, P.G., 2007. Sinter-vein correlations at Buckskin Mountain, National District, Humboldt County, Nevada. *Econ. Geol.* 102, 193–224.
- Walter, M.R., 1972. A hot spring analog for the depositional environment of Precambrian iron formations of the Lake Superior region. *Econ. Geol.* 67, 965–980.
- Walter, M.R., 1976. Hot-spring sediments in Yellowstone National Park. In: Walter, M.R. (Ed.), *Stromatolites*. Elsevier, Amsterdam, pp. 489–498.
- Walter, M.R., Bauld, J., Brock, T.D., 1976. Microbiology and morphogenesis of columnar stromatolites (*Conophyton*, *Vaccerrilla*) in Yellowstone National Park. In: Walter, M.R. (Ed.), *Stromatolites*. Elsevier, Amsterdam, pp. 273–310.
- Walter, M.R., Des Marais, D., Farmer, J.D., Hinman, N.W., 1996. Lithofacies and biofacies of mid-Paleozoic thermal spring deposits in the Drummond Basin, Queensland, Australia. *Palaios* 11, 497–518.
- Weed, W.H., 1889. The diatom marshes and diatom beds of the Yellowstone National Park. *Bot. Gaz.* 117–120 (May).
- White, N.C., Hedenquist, J.W., 1990. Epithermal environments and styles of mineralization; variations and their causes, and guidelines for exploration. *J. Geochem. Explor.* 36, 445–474.
- White, N.C., Wood, D.G., Lee, M.C., 1989. Epithermal sinters of Paleozoic age in north Queensland, Australia. *Geology* 17, 718–722.
- Yoshimura, K., Liu, Z., Cao, J., Yuan, D., Inokura, Y., Noto, M., 2004. Deep source CO₂ in natural waters and its role in extensive tufa deposition in the Huanglong Ravines, China. *Chem. Geol.* 205, 141–153.
- Zimmerman, B.S., Larson, P.B., 1994. Epithermal gold mineralization in a fossil hot spring system, Red Butte, Oregon. *Econ. Geol.* 89, 1983–2002.